Title

Detection of Multiple Sclerosis Biomarkers in Serum by Ganglioside Microarrays and Surface Plasmon Resonance Imaging.

Journal

ACS Sensors, 5(11)

Authors

Malinick, Alexander

Lambert, Alexander

Stuart, Daniel

et al.

Publication Date

2020-11-25

DOI

10.1021/acssensors.0c01935

Peer reviewed

HHS Public Access

Author manuscript

ACS Sens. Author manuscript; available in PMC 2021 August 18.

Published in final edited form as:

ACS Sens. 2020 November 25; 5(11): 3617–3626. doi:10.1021/acssensors.0c01935.

Detection of Multiple Sclerosis Biomarkers in Serum by Ganglioside Microarrays and Surface Plasmon Resonance Imaging

Alexander S. Malinick[†], **Alexander S. Lambert**[†], **Daniel D. Stuart**[†], **Bochao Li**[‡], **Ellie Puente**[†], **Quan Cheng**[†,‡,*]

[†]Department of Chemistry, University of California, Riverside, CA 92521, USA

[‡]Environmental Toxicology, University of California, Riverside, CA 92521, USA

Abstract

Multiple sclerosis (MS) is an autoimmune disease that damages the myelin sheaths of nerve cells in the central nervous system (CNS). An individual suffering from MS produces increased levels of antibodies that target cell membrane components, such as phospholipids, gangliosides, and membrane proteins. Among them, anti-ganglioside antibodies are considered important biomarkers to differentiate MS from other diseases that exhibit similar symptoms. We report here a label-free method for detecting a series of antibodies against gangliosides in serum by surface plasmon resonance imaging (SPRi) in combination with a carbohydrate microarray. The ganglioside array was fabricated with a plasmonically tuned, background-free biochip, and coated with a perfluorodecyltrichlorosilane (PFDTS) layer for antigen attachment as a self-assembled pseudo-myelin sheath. The chip was characterized with AFM and MALDI-MS, demonstrating effective functionalization of the surface. SPRi measurements of patient mimicking blood samples were conducted. A multiplexed detection of antibodies for anti-GT_{1b}, anti-GM_1, and anti-GA_1 in serum was demonstrated, with a working range of 1 ng/mL to 100 ng/mL, suggesting it is well suited for clinical assessment of antibody abnormality in MS patients. Statistical analyses including PLS-DA and PCA show the array allows comprehensive characterization of cross reactivity patterns between the MS specific antibodies, and can generate a wide range of information compared to traditional end point assays. This work uses PFDTS surface functionalization and enables direct MS biomarker detection in serum, offering a powerful alternative for MS assessment and potentially improved patient care.

Graphical Abstract

[*]Corresponding author: Quan Cheng, Tel: (951) 827-2702, Fax: (951) 827-4713, quan.cheng@ucr.edu.

Supporting Information:

The supporting information is available free of charge at ACS Publications website.

Contact angles for PFDTS, 0.1 mg/mL GT_{1b}, 0.1 mg/mL GA_1, and 0.1 mg/mL GM_1 surfaces, MALDI-MS results for GA_1 and GM_1 gangliosides on SPRi ganglioside microarray after exposure to microfluidic conditions, AFM of silica gold surface before and after polymerization with PFDTS, cartoon diagram of modified fabrication procedure for SPRi microarray biochips (PDF).

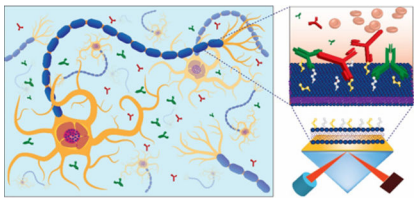

Keywords

Multiple sclerosis; gangliosides; microarray; serum biomarkers; surface plasmon resonance; SPR imaging

It is estimated that almost two million people are affected by multiple sclerosis (MS) worldwide, but the true number of MS patients remains unknown due to the difficulty of obtaining an accurate diagnosis.[1] Although there have been attempts to link MS to genetics, environmental conditions, dietary restrictions, or viruses as the underlying factors that lead to its development, many of these studies have proved to be inconclusive.[1, 2] While the underlying causes of MS remain elusive, the process by which the symptoms associated with MS are displayed is well understood.[3] The most common symptoms observed in MS patients are numbness, slurred speech, paralysis, vertigo, impotence, tremors, loss of muscle control, and change in or loss of vision.[4] These symptoms have been directly associated with damage to the myelin sheath in the nervous system. The myelin sheath is a lipid rich material: 0.3 % of which are gangliosides, 15 to 30 % are various proteins, and the remaining 70 to 85 % are various lipids.[5] Gangliosides are sialic acid-containing glycosphingolipids and are essential for cell-cell recognition, adhesion, and signal transduction throughout the CNS.[6] In MS patients, the concentrations of anti- ganglioside antibodies in serum range between 3 ng/mL to 20 ng/mL.[7] These antibodies may initiate the attack on myelin sheaths as well as oligodendrocytes, which leads to demyelination. A number of symptoms in MS have been suggested to be associated with specific anti-ganglioside antibodies.[8] For instance, anti-GA_1 and anti-GM_1 have been linked to optic nerve damage resulting in symptoms associated with eye movement and inflammation, while anti-GT_{1b} is believed to be associated with loss of muscle control, specifically in the upper and lower limbs.[9–12]

Current diagnostic techniques for MS are considered to be inconsistent and unreliable.[13] This is primarily due to the variation of symptoms expressed from patient to patient. Magnetic resonance imaging (MRI) and electrophysiologic recordings are often used in tandem to assess whether an autoimmune attack has occurred and caused damage to the CNS.[14–16] To further confirm the diagnosis, blood tests and spinal taps are then conducted to rule out other diseases that show similar symptoms.[16, 17] Spinal taps or lumbar punctures are employed to collect cerebrospinal fluid (CSF) for elevated levels of autoimmune antibodies, oligoclonal bands, and white blood cells.[18, 19] While lumbar punctures facilitate the detection of MS, it is an unattractive avenue for disease progression monitoring due to limited sample size that can be extracted, difficulty in performing the procedure, and the inability to routinely collect CSF.[19] The last issue proves to be a major hurdle since accurate diagnosis through these methods can range anywhere between a few

months to several years.[20] Blood tests thus have gained considerable interest in recent years as a way to detect and monitor the progression of MS due to their quick and minimally invasive collection procedure. Unlike lumbar punctures, blood samples can be easily collected in large quantities and at different timepoints. However, common biomarkers often have much lower concentrations in blood than in CSF, which is the reason why highly sensitive detection is urgently needed.[17, 21–24] While there currently is no definitive blood test that allows unambiguous MS diagnosis, these tests are routinely conducted to determine if other diseases may be present that have similar symptoms as MS. It should be noted that the common blood biomarker tests intended for MS diagnosis also include those markers for Lyme disease, rare hereditary disorders, syphilis, HIV/AIDS, lupus, and fibromyalgia.[17, 21–23] ELISA has been the method of choice for antibody detection and serologic diagnosis. The CDC has called for the development of new tests of these markers in an advanced format that can be more informative. Microarray technology is capable of detecting antibodies at biologically relevant concentrations and under identical testing conditions, which would give new insights into which antibodies are linked to specific inflammation and damage to the CNS. The microarray test of anti- ganglioside antibodies and a quantitative assessment of their cross reactivity could also simplify the diagnostic procedure, combining the benefits of blood tests and spinal taps for effective detection, characterization, and evaluation of MS.

In this work, we report a multiplexed detection for a series of MS biomarkers in serum by using surface plasmon resonance imaging (SPRi) in combination with ganglioside microarrays (Figure 1). SPRi is a label free, real time, sensitive and direct detection method,[25] and has found broad applications in drug delivery,[26] cell based analysis,[27] biomarker profiling,[28] and biotechnology.[29] The ganglioside array used in this work was built with plasmonically tuned, background-free biochips and a coating of a perfluorodecyl-trichlorosilane (PFDTS) monolayer. PFDTS is a near superhydrophobic agent that forms compact monolayers on silica coatings on our SPR chips, which exhibits antifouling properties[30] and allows simple functionalization with gangliosides (Figure 1C). Three gangliosides (GA_1, GM_1, and GT_{1b}), structures of which are shown in Figure 1B, were chosen for this work and incorporated into the PFDTS microarray that mimic the myelin sheath. These gangliosides were chosen for initial test because antibodies for these antigens are pathologically relevant and are associated with common MS symptoms such as rapid eye movement, loss or change of vision, and loss of upper and lower muscle control.[8–12] Once verified, this microarray method can expand and include additional gangliosides for a more comprehensive testing.

EXPERIMENTAL METHODS:

Materials and Reagents:

1H,1H,2H,2H-Perfluorodecyltrichlorosilane (PFDTS) was obtained from Fisher Scientific (Pittsburgh, PA). Monoganglioside GM_1 was obtained from Matreya (Pleasant Gap, PA). Trisialoganglioside GT_{1b} was purchased from Biosynth (Itsaca, Il). Anti monoganglioside GM_1 rabbit polyclonal antibody, anti asialoganglioside GA_1 human anti mouse monoclonal antibody were purchased from Abcam (Cambridge, UK). Anti Trisialoganglioside GT_{1b}

ganglioside mouse monoclonal antibody was purchased from Millipore Sigma (Billerica, MA). Asialoganglioside GA_1, anti Trisialoganglioside anti-GT_{1b} antibody heavy chain specific human anti mouse monoclonal antibody, α-cyano-4- hydroxycinnamic acid (CHCA) were from Sigma-Aldrich (St. Louis, MO). Human serum was purchased from Innovative Research (Upper Marlboro, MD).

Fabrication of SPR and SPRi Substrates:

Fabrication of SPR and SPRi chips was performed following a previous procedure published by our group.[31] In brief, 2 nm of titanium (0.5 Å/s) followed by 48 nm of gold (2.0 Å/s), were deposited on slides via electron beam physical vapor deposition (EBPVD) (Temescal, Berkeley, CA). This is followed by depositing roughly 1–3 nm of SiO_2 onto the gold layer via plasma enhanced chemical vapor deposition (PECVD) using a Unaxis Plasmatherm 790 system (Santa Clara, CA). For SPRi arrays, the slides were spin-coated with hexamethyldisilazane (HMDS) to promote adhesion with AZ5214E at 4000 rpm for 45 s. After baking at 110 °C for approximately 1 minute, UV exposure via a Karl- Suss MA- 6 system was used to create an array pattern on the photoresist, which was followed by standard photoresist development protocols. The well walls were formed by a 2 nm layer of titanium as an adhesion layer followed by 200 nm of gold both deposited via EBPVD. The remaining photoresist was lifted from the surface with acetone. Once all the wells were removed, another layer of 2 nm of titanium was deposited followed by 48 nm of gold both deposited via EBPVD to form the sensing surface inside of the wells. PECVD was then used to deposit 1–3 nm of SiO_2 on the microarray chips. The SPRi microarray chips consisted of 10 × 10 well arrays that were 600 μm in diameter and 200 nm deep.

Surface Functionalization and Preparation:

For functionalization, the chips were submerged in 1 mM PFDTS that was diluted in toluene. After 30 minutes, the chip was removed from the solution and rinsed with toluene, ethanol, and deionized water and dried with nitrogen gas. Once the chips were dry, 20 μL of 100 μg/mL GA_1, GM_1, or GT_{1b} gangliosides in chloroform were pipetted onto the chips and covered with a glass cover slip to allow the gangliosides to evenly cover the SPR chips surface. The chips were then allowed to dry for 5 minutes under ambient conditions. For SPRi chips, 1.5 μL of the 100 μg/mL stock solution for each ganglioside were incubated into each well of their respective row to create four different working channels (eight working wells per channel) when attached to the PDMS flow cell. Each chip was fabricated using the same configuration: the first channel is left non-functionalized as an internal standard to determine chip to chip variation, while 1 μL of 100 μg/mL stock solutions of GA_1, GM_1, and GT_{1b} gangliosides are pipetted onto each well and left to dry.

Microarray Surface Characterization

The biochips were further characterized at various fabrication steps via AFM. The SPR biochips were examined during each functionalization step: first silica gold (Au), then PFDTS silica Au, and finally GT_{1b} ganglioside functionalized onto the PFDTS silica Au biochip. GT_{1b} ganglioside was used as a representative of the gangliosides to confirm that they form evenly onto the surface. Contact angle measurements were used to determine the hydrophobicity of the surfaces at various fabrication steps.[32] All images were taken at

ambient temperature and pressure. MALDI-MS instrument was used to confirm the presence and identity of gangliosides on the array after functionalization. A MALDI matrix of 1 mL CHCA was prepared with 50 % acetonitrile, 49 % DI H_2O, and 1 % trifluoroacetic acid. For the SPRi multiplexed biochips, 1 μL of matrix solution was pipetted into each well and allowed to dry. Chips were mounted on a steel MALDI plate and analyzed with an AB SCIEX TOF/TOF 5800 spectrometer operating in negative ion reflector mode at an intensity of 5000 A.U.

SPR and SPRi analysis:

A NanoSPR5–321 (NanoSPR, Chicago, IL), a dual-channel SPR spectrometer with a GaAs semiconductor laser light source set at a wavelength of 670 nm, was used for all spectroscopic measurements for conventional SPR biosensing. The device utilizes a prism with refractive index of n=1.61 and a 30 μL flow cell. PBS (phosphate buffered saline) running buffer at a pH of 7.4 was used in all experiments with a flow speed of 5 mL/h. Solutions of anti-GA_1, anti-GM_1, and anti-GT_{1b} were diluted with 1 × PBS to various concentrations for SPR experiments. After injection into the devices, solutions were incubated for 30 minutes before rinsing. In serum experiments anti-GT_{1b} was spiked into 10 % human serum diluted with PBS.

SPRi measurement was conducted on a home-built setup and a detailed description of which can be found in our previous work.[33] The functionalized substrates were mounted onto an optical stage that houses a PDMS flow cell. The array was placed in contact with an equilateral SF2 prism (n = 1.65) with a layer of refractive index matching fluid (Cargill Laboratories, Cedar Grove, NJ). A 648 nm light emitting diode (LED) was used as the light source for SPR excitation. Reflected images of the microarray were captured by a cooled 12- bit CCD camera (QImaging Retiga 1300) and data acquisition was controlled via a home built LabView program. Intensity data was normalized by using the intensity from the *p*-polarized light over the *s*-polarized beam and described as a percentage.

Statistical analysis:

Analysis of variance (ANOVA) was conducted in Excel with the Analysis ToolPak add-in and used the end point data obtained with SPRi. Partial least squares discrimination analysis (PLS-DA) plots were generated with MetaboAnalyst platform and used the raw data from the SPRi sensorgrams for analysis. Principal component analysis (PCA) was completed with the prcomp function in R and graphed with the ggbiplot package with an ellipse probability set to 95 % using the end point data from the SPRi ganglioside microarray data.

RESULTS AND DISCUSSION:

Biochip Surface Fabrication and Characterization

Perfluorinated hydrocarbon monolayers have been reported as an attractive surface for detection of analytes in complex media due to their near superhydrophobic and antifouling properties.[34] The monolayer can interact strongly with hydrophobic tags or moieties that are attached to the probes, presenting the antigenic sensing site in a well-organized and easy to access manner.[34] This works ideally for ganglioside immobilization and formation

of ganglioside microarrays (Figure 1). We generated the PFDTS monolayer on a silica coating of the gold SPR substrate, where the silica nanofilm can also improve plasmonic properties for binding interactions.[35] Confirmation of ganglioside immobilization on the biochips was achieved by contact angle measurement, AFM, and MALDI-MS. Contact angle measurement shows that the pristine silica surface had a contact angle of 64.0 ± 2.0 degrees, indicating that the surface is rather hydrophilic (Figure 2 insertion). After PFDTS coating, the contact angle drastically increased to 131.1 ± 2.5 degrees; this value is close to what is accepted as being a superhydrophobic surface.[33] Three different gangliosides were used to make the array: GA_1, GM_1, and GT_{1b}. After incubating, the contact angles for the ganglioside functionalized surfaces were 125.9 ± 3.1, 125.9 ± 2.3, and 124.9 ± 3.9 degrees, respectively (Figure S1). The results also showed that the functionalized PFDTS substrate maintained hydrophobicity after the ganglioside deposition. This is important to the sensing in complex media as highly hydrophobic surfaces have been shown to play significant roles in antifouling techniques.[30, 36]

MALDI-MS was conducted to confirm that ganglioside functionalization onto the PFDTS surface was successful and remained after washing under microfluidic conditions. The MS spectra for GT_{1b} ganglioside is shown in Figure 2A, as it fragments into the other gangliosides of interest in this study. Peaks used for the confirmation that GT_{1b} ganglioside was on the surface were 2158.91 m/z, 2129.98 m/z, and 2108.92 m/z.[37, 38] During the ionization process it is possible for $GT1_b$ ganglioside to fragment and lose its sialic acid (SA) groups.[37] The fragmentation of GT_{1b} splits it into one SA and either $GD1_a$ or $GD1_b$, which are both associated with the peaks at 1863.82 m/z and 1835.77 m/z.[37, 38] Because $GD1_a$ and $GD1_b$ gangliosides both have the same mass and the difference between the two is the location of the SA groups, they cannot be differentiated by the presented spectra. Fragmentation continues with the loss of a second SA groups resulting in GM_1 associated peaks 1572.77 m/z and 1544.75 m/z being present.[37, 38] The loss of the third and final SA group from the fragmented GT_{1b} ganglioside results in the peaks associated with GA_1 ganglioside being present which are 1270.30 m/z and 1252.29 m/z.[38] The collected results agree well with the spectra found in literature. GT_{1b} associated peaks range from 2150 to 2250 m/z, $GD1_a$ and $GD1_b$ range between 1800 to 1900 m/z, GM_1 confirmed peaks are from 1500 to 1600 m/z, and GA_1 associated peaks range between 1200 to 1300 m/z.[37–41] The MS spectra for GM_1 and GA_1 gangliosides can be found in the Supplemental Information (Figures S2–S3).

AFM was also utilized to characterize the surface at various fabrication steps: silica gold chip, PFDTS monolayer on silica gold, and ganglioside on PFDTS on the silica gold chip (Figure 2 C–D and Supporting Materials). Surface roughness was measured for each fabrication step to ensure no clumping had occurred, which could potentially compromise the sensitivity on both SPR and SPRi. GT_{1b}, the largest ganglioside in the group, was used as a representative ganglioside for array fabrication characterization. The RMS for the silica gold surface, PFDTS monolayer on the silica gold surface, and GT_{1b} ganglioside functionalized PFDTS monolayer were 1.63 nm, 10.47 nm, and 9.34 nm, respectively. The deposited layers did not appear to agglomerate in specific regions on the chip at any of the fabrication steps, and that the surfaces were in fact smooth. While there is a moderate increase in surface roughness for the functionalized surfaces, the values still fall well below

the decay length of the SPR evanescent field, suggesting that the PFDTS functionalization has little effect on sensing performance.[42]

Capture of Antibodies on Ganglioside Functional Surfaces by Spectroscopic SPR

Conventional SPR biosensing was initially used to characterize the antibody binding to the functionalized biochips before attempting multiplexed detection on an SPRi instrument. All experiments were conducted with antibodies diluted in PBS to measure specific binding on their respective surfaces as well as nonspecific binding and cross reactivity between various antibodies. To account for cross reactivity between the ganglioside surface and the anti-ganglioside specific antibody, the antibody that showed the highest nonspecific binding was used as a control. Figure 3A shows the sensorgrams where 50 ng/mL of anti-GM_1 and anti-GA_1 were injected onto a 0.1 mg/mL GA_1 ganglioside surface. This process was also performed on the GT_{1b} ganglioside surface with 10 ng/mL of anti-GT_{1b} and 10 ng/mL of anti-GA_1 (Figure 3B). In both cases, a baseline was quickly established, and the control antibody had little to no binding to the surface. This is in direct contrast to the specific antibody/ganglioside pair (Figure 3. A and B lower curves), which shows a clear angular shift, even after the rinse cycle.

A calibration curve for the three antibodies was generated at concentrations ranging from 1–100 ng/mL, as shown in Figure 3C. From the sensorgrams, the specific binding of 10 ng/mL of anti-GT_{1b} on a GT_{1b} ganglioside surface has roughly the same specific binding as a 25 ng/mL anti-GM_1 on a GM_1 ganglioside surface. The reported LOD, calculated by using the 3σ method, were 17.6 ng/mL for anti-GA_1, 11.3 ng/mL for anti-GM_1, and 8.2 ng/mL for anti-GT_{1b}, respectively. The stronger binding interactions and lower LOD observed for anti-GT_{1b} can be attributed to the large headgroup (more sialic acids) of GT_{1b} ganglioside.[43] We thus chose anti-GT_{1b} as the model biomarker for the assessment of MS specific antibodies in serum at biologically relevant concentrations using SPRi.

SPR Imaging Detection of Anti-GT_{1b} in Serum

SPRi allows interrogation of multiple elements simultaneously and thus provides real time analysis with the additional benefit of high throughput and multiplexed detection.[28] Previous work in our lab demonstrated that patterned gold substrate with microwells yielded arrays with tunable plasmonic properties for various experimental needs.[44] And a background free imaging analysis with enhanced sensitivity and contrast can be realized.[28, 31, 45] This property was combined with the PFDTS monolayer and gangliosides for SPRi detection of MS related antibodies in serum in this work (Figure 4). We modified slightly the array fabrication procedure for attenuating background plasmonics[31, 46] (Figure S6), and introduced an alkyltrichlorosilane-based procedure for surface modification.[34] The PFDTS coating yielded a relatively ordered surface to enable strong hydrophobic-hydrophobic interactions, and the coating does not compromise surface smoothness and thus the performance, as discussed previously.

Using a loop flow cell, 4 working channels were defined in the microarray analysis; each channel having eight active wells for statistical analysis, as shown in Figure 4. There was an unfunctionalized channel (framed in black) that was used as a reference point to account for

chip to chip variation. The response of anti-GT_{1b} on the ganglioside array, when specifically detecting anti-GT_{1b}, showed a low signal of nonspecific binding in the diluted serum. The collected results show excellent agreement with the collected data on spectroscopic SPR (Figure 3C) and SPRi biosensing in other buffering conditions such as PBS and 2.0 mg/mL BSA (Figure 6).

Nonspecific binding from complex media onto the sensing interface for SPR and SPRi is arguably the major factor that hinders wide utilization of SPR detection methods as a routine diagnostic tool.[45, 47] To further characterize the nonspecific binding on the PFDTS layer, we saturated the surface with 10 % serum before antibody injection and evaluated the sensing performance (Figure 5A). The serum acts as an antifouling agent by blocking nonspecific binding locations that may become occupied when the anti-GT_{1b} spiked serum samples are introduced. 10 % serum was selected to passivate the surface as this was the same dilution that the antibodies were spiked into and 10 % serum has been used to represent complex media in literature.[48] To characterize specific detection of anti-GT_{1b} and monitor cross reactivity, we tested antibodies at various concentrations (1 ng/mL to 100 ng/mL) and compared the response. A typical sensorgram is shown in Figure 5B, which shows low cross reactivity of anti-GM_1 on a GT_{1b} ganglioside surface. The shift caused by 100 ng/mL anti-GT_{1b} was much larger than that by 100 ng/mL anti-GM_1 on a $GT1_{1b}$ ganglioside surface, indicating specific binding and also some level of cross reactivity. After rinsing the surface with PBS, the signal for anti-GT_{1b} was again higher than for anti-GM_1, which agrees with the results on spectroscopic SPR.

A calibration curve for anti-GT_{1b} under different experimental conditions was generated using SPRi data, as shown in Figure 6. The sensing surface has a working range of 1 ng/mL to 100 ng/mL. The LOD was calculated to be 2.34 ng/mL using the 3σ principle. The results showed that this ganglioside microarray is capable of detecting MS antibodies in serum at clinically relevant levels, which are present in patient serum at concentrations between 3 ng/mL and 20 ng/mL.

Multiplexed Detection and Statistical Analysis of Ganglioside Antibodies in Serum

Precise detection of various antibodies for MS-related gangliosides in serum is a complex process due to existence of cross reactions. We used hydrocarbon microarray to investigate the cross reactivity with the multiplexed detection of anti-GT_{1b}, anti-GM_1, and anti-GA1 in 10 % human serum (Figure 7). The data presented was the average of at least 5 samples, and 0.1 mg/mL of GA_1, GM_1, and GT_{1b} ganglioside were used for microarray fabrication. The shifts caused by 100 ng/mL anti-GT_{1b} were 0.66 ± 0.23 % RIU on GA_1 surface, 1.21 ± 0.10 % RIU on GM_1 surface, and 4.62 ± 0.24 % RIU on GT_{1b} surface. The results indicate that anti-GT_{1b} shows the largest response for its ganglioside, indicating the selectivity of the antibody and also suggesting elevated binding strength due to a large headgroup.[43] The shifts caused by 100 ng/mL anti-GM_1 on the GA_1, GM_1, and $GT1_b$ microarray were 1.62 ± 0.21 % RIU, 3.35 ± 0.17 % RIU, and 0.98 ± 0.23 % RIU respectively, while 100 ng/mL of anti-GA_1 caused a shift that resulted in a 3.32 ± 0.17 % RIU for GA_1, 1.25 ± 0.23 % RIU for GM_1, and 0.58 ± 0.17 % RIU for GT_{1b}. Using the lowest binding as a correction for nonspecific binding, we calculated the specific binding for the three antibodies in spiked

serum to be 3.64 ± 0.24 % RIU, 2.01 ± 0.17 % RIU, and 1.70 ± 0.17 % RIU for anti-GT_{1b}, anti-GM_1, and anti-GA_1, respectively. The cross reactivity between anti-GM_1 and anti-GA_1 can be attributed to the similar structure of the two gangliosides, where the only difference is that GM_1 has a SA group while GA_1 does not.[49]

To further evaluate the cross reactivity and differentiate antibody-ganglioside interactions, we conducted several statistical analyses of the microarray data including analysis of variance (ANOVA), partial least squares discriminant analysis (PLS-DA), and principal component analysis (PCA). ANOVA indicated antibody interactions with different ganglioside surfaces are statistically relevant with calculated p-values ≤ 0.05. The variance was found to vary between 0.06 and 0.03, with anti-GT_{1b}/GT_{1b} pair having the lowest variance while anti-GA_1/GA_1 having the highest variance. PLS-DA was conducted using longer range of data from the SPRi sensorgrams, which allowed for evaluation of the binding interactions that include both kinetic and steady state components. PLS-DA results indicated marked differences for anti-GT_{1b} and anti-GA_1 as the gangliosides differ the most. Figure 7B shows the score plot for anti-GA_1 binding associations with each ganglioside on the array. There was a substantial overlap between anti-GA_1 and GM_1 ganglioside, whereas no overlap was observed between anti-GA_1 and GT_{1b} ganglioside. Interactions of anti-GT_{1b} with various gangliosides on the array is shown in Figure 7C. As expected, anti-GT_{1b} and GM_1 ganglioside had some cross reactivity while no overlap was present for GA_1 ganglioside. The cross reactivity observed agrees well with data collected on conventional SPR (Figure 3A–B) and on SPRi (Figure 4A), and can be attributed to the presence of SA group(s). The larger structural difference between GT_{1b} and GA_1 decreases the cross reactivity, while this effect appears to be reversed for similar structures of GM_1 and GA_1. The analysis with PLS-DA using binding kinetic features allows determination of the extent of cross reactivity and selectivity of the antibodies. This approach may provide highly useful information on the nature of the immune interactions between structurally similar antigens.

In addition, PCA analysis was conducted based on end point values for each array component, as shown in Figure 7D. A clear separation between anti-GT_{1b}, anti-GM_1, and anti-GA_1 regions is obtained, which agrees well with the calibration curves in Figure 3C. This ability to identify specific antibody/ganglioside interaction is very significant, because it shows the microarray method is powerful for differentiating multiple antibodies in a single experiment, even with an extensive degree of cross reactivity.

These statistical analyses provide convincing evidence that the functionalized PFDTS ganglioside microarray is capable of probing the complex cross reactivity network between the MS specific antibodies, and is thus able to provide a wide range of information compared to traditional end point assays. The effectiveness of the microarray can be attributed to the near superhydrophobic properties of the PFDTS surface, the carbohydrate head groups of the probes, and the added surface protection techniques. The array can also allow for high throughput antibody screening for disease diagnosis in patient samples, which may lead to faster diagnosis and more effective therapies.

Conclusion:

We have demonstrated a new and effective platform to screen blood samples for potential diagnosis of multiple sclerosis by assessing ganglioside antibody interactions and quantifications. The SPRi microarray biochip has shown to be able to detect and differentiate between MS specific antibodies at biological relevant concentrations. This method is an important step towards MS diagnosis as the complexity of MS is partially attributed to the clinical observation of high individual heterogeneity that certain antibodies present in one patient may not be expressed in another, and the concentrations may vary wildly. Therefore, detecting a broad range of antibodies with multiplexed capability and under identical assay conditions is critical. The ganglioside microarray can be easily extended to include other important glycolipids and sphingomyelins from the myelin sheath, which will allow for a broad-spectrum profiling of the patients' samples. Using anti-GT_{1b} as an example, we showed this microarray can detect biomarkers within the range of disease relevant concentrations of 3 ng/mL to 25 ng/mL. Statistical analysis presented here using ANOVA, PLS-DA, and PCA allowed for the analysis of features in the SPRi sensorgrams and the endpoint data, revealing unique characteristics that can be used for identification of specific analyte/antigen interactions. We believe the work presented here has the potential to improve disease diagnosis, enhance the evaluation of disease progression, and may lead to improvements in drug development that aims at blocking antigen binding regions and inhibiting the immune system from targeting components of the CNS. Future work will expand to cover more immuno biomarkers in whole serum and inclusion of signal amplification for detecting those potential biomarkers with extremely low abundance.

Supplementary Material

Refer to Web version on PubMed Central for supplementary material.

Acknowledgements:

The authors acknowledge support from the National Institute of Health (R21AI140461). A.S.L. was supported by an NIEHS T32 training grant (T32-ES018827).

Reference:

1. Goldenberg MM, Multiple sclerosis review. Pharmacy and Therapeutics2012, 37 (3), 175. [PubMed: 22605909]
2. Organization WH, Atlas: multiple sclerosis resources in the world 2008. 2008.
3. Compston A; Coles A, Multiple sclerosis. Lancet2002, 359 (9313), 1221–31. [PubMed: 11955556]
4. Polman CH; Reingold SC; Edan G; Filippi M; Hartung HP; Kappos L; Lublin FD; Metz LM; McFarland HF; O'Connor PW; Sandberg-Wollheim M; Thompson AJ; Weinshenker BG; Wolinsky JS, Diagnostic criteria for multiple sclerosis: 2005 revisions to the "McDonald Criteria". Ann Neurol2005, 58 (6), 840–6. [PubMed: 16283615]
5. Brady S; Siegel G; Albers RW; Price D, Basic neurochemistry: molecular, cellular and medical aspects. Elsevier: 2005.
6. Schnaar RL, Brain gangliosides in axon–myelin stability and axon regeneration. FEBS letters2010, 584 (9), 1741–1747. [PubMed: 19822144]
7. Koutsouraki E; Hatzifilippou E; Cosetsidou C; Avdelidi E; Banaki T; Costa V; Baloyannis S, Anti-GM1 antibodies in multiple sclerosis patients: P2674. European Journal of Neurology2008, 15.

8. Reindl M; Khalil M; Berger T, Antibodies as biological markers for pathophysiological processes in MS. Journal of neuroimmunology2006, 180 (1–2), 50–62. [PubMed: 16934337]

9. Hogan EL; Podbielska M; O'Keeffe J, Implications of lymphocyte anergy to glycolipids in multiple sclerosis (MS): iNKT cells may mediate the MS infectious trigger. Journal of clinical & cellular immunology2013, 4 (3).

10. Marconi S; Acler M; Lovato L; De Toni L; Tedeschi E; Anghileri E; Romito S; Cordioli C; Bonetti B, Anti-GD2-like IgM autoreactivity in multiple sclerosis patients. Multiple Sclerosis Journal2006, 12 (3), 302–308. [PubMed: 16764343]

11. Pender MP; Csurhes PA; Wolfe NP; Hooper KD; Good MF; McCombe PA; Greer JM, Increased circulating T cell reactivity to GM3 and GQ1b gangliosides in primary progressive multiple sclerosis. Journal of clinical neuroscience2003, 10 (1), 63–66. [PubMed: 12464524]

12. Mizutani K; Oka N; Kusunoki S; Kaji R; Mezaki T; Akiguchi I; Shibasaki H, Sensorimotor demyelinating neuropathy with IgM antibody against gangliosides GD1a, GT1b and GM3. Journal of the neurological sciences2001, 188 (1–2), 9–11. [PubMed: 11489278]

13. Brownlee WJ; Hardy TA; Fazekas F; Miller DH, Diagnosis of multiple sclerosis: progress and challenges. The Lancet2017, 389 (10076), 1336–1346.

14. Traboulsee A; Simon J; Stone L; Fisher E; Jones D; Malhotra A; Newsome S; Oh J; Reich D; Richert N, Revised recommendations of the consortium of MS centers task force for a standardized MRI protocol and clinical guidelines for the diagnosis and follow-up of multiple sclerosis. American Journal of Neuroradiology2016, 37 (3), 394–401. [PubMed: 26564433]

15. Laufs H; Daunizeau J; Carmichael DW; Kleinschmidt A, Recent advances in recording electrophysiological data simultaneously with magnetic resonance imaging. Neuroimage2008, 40 (2), 515–528. [PubMed: 18201910]

16. McDonald WI; Compston A; Edan G; Goodkin D; Hartung HP; Lublin FD; McFarland HF; Paty DW; Polman CH; Reingold SC, Recommended diagnostic criteria for multiple sclerosis: guidelines from the International Panel on the diagnosis of multiple sclerosis. Annals of Neurology: Official Journal of the American Neurological Association and the Child Neurology Society2001, 50 (1), 121–127.

17. Solomon AJ; Bourdette DN; Cross AH; Applebee A; Skidd PM; Howard DB; Spain RI; Cameron MH; Kim E; Mass MK, The contemporary spectrum of multiple sclerosis misdiagnosis: a multicenter study. Neurology2016, 87 (13), 1393–1399. [PubMed: 27581217]

18. Robinson WH; DiGennaro C; Hueber W; Haab BB; Kamachi M; Dean EJ; Fournel S; Fong D; Genovese MC; De Vegvar HEN, Autoantigen microarrays for multiplex characterization of autoantibody responses. Nature medicine2002, 8 (3), 295–301.

19. Derkus B; Bozkurt PA; Tulu M; Emregul KC; Yucesan C; Emregul E, Simultaneous quantification of Myelin Basic Protein and Tau proteins in cerebrospinal fluid and serum of Multiple Sclerosis patients using nanoimmunosensor. Biosensors and Bioelectronics2017, 89, 781–788. [PubMed: 27816592]

20. Frohman E; Havrdova E; Lublin F; Barkhof F; Achiron A; Sharief M; Stuve O; Racke M; Steinman L; Weiner H, Most patients with multiple sclerosis or a clinically isolated demyelinating syndrome should be treated at the time of diagnosis. Archives of neurology2006, 63 (4), 614–619. [PubMed: 16606781]

21. Solomon AJ; Weinshenker BG, Misdiagnosis of multiple sclerosis: frequency, causes, effects, and prevention. Current neurology and neuroscience reports2013, 13 (12), 403. [PubMed: 24142849]

22. Solomon AJ; Corboy JR, The tension between early diagnosis and misdiagnosis of multiple sclerosis. Nature Reviews Neurology2017, 13 (9), 567–572. [PubMed: 28799551]

23. Solomon AJ; Klein EP; Bourdette D, "Undiagnosing" multiple sclerosis: the challenge of misdiagnosis in MS. Neurology2012, 78 (24), 1986–1991. [PubMed: 22581930]

24. Boissy AR; Ford PJ, A touch of MS: therapeutic mislabeling. Neurology2012, 78 (24), 1981–1985. [PubMed: 22581929]

25. Kodoyianni V, Label-free analysis of biomolecular interactions using SPR imaging. Biotechniques2011, 50 (1), 32–40. [PubMed: 21231920]

26. He Y; Yang M; Zhao S; Cong C; Li X; Cheng X; Yang J; Gao D, Regulatory mechanism of localized surface plasmon resonance based on gold nanoparticles-coated paclitaxel nanoliposomes

and their antitumor efficacy. ACS Sustainable Chemistry & Engineering2018, 6 (10), 13543–13550.

27. Kreysing E; Hassani H; Hampe N; Offenhäusser A, Nanometer-Resolved Mapping of Cell–Substrate Distances of Contracting Cardiomyocytes Using Surface Plasmon Resonance Microscopy. ACS nano2018, 12 (9), 8934–8942. [PubMed: 30180539]
28. Lambert A; Yang Z; Cheng W; Lu Z; Liu Y; Cheng Q, Ultrasensitive detection of bacterial protein toxins on patterned microarray via surface plasmon resonance imaging with signal amplification by conjugate nanoparticle clusters. ACS sensors2018, 3 (9), 1639–1646. [PubMed: 30084634]
29. Nguyen HH; Park J; Kang S; Kim M, Surface plasmon resonance: a versatile technique for biosensor applications. Sensors2015, 15 (5), 10481–10510. [PubMed: 25951336]
30. Banerjee I; Pangule RC; Kane RS, Antifouling coatings: recent developments in the design of surfaces that prevent fouling by proteins, bacteria, and marine organisms. Advanced materials2011, 23 (6), 690–718. [PubMed: 20886559]
31. Abbas A; Linman MJ; Cheng Q, Patterned resonance plasmonic microarrays for high-performance SPR imaging. Analytical chemistry2011, 83 (8), 3147–3152. [PubMed: 21417424]
32. Duan J; Wang H; Cheng Q, On-plate desalting and SALDI-MS analysis of peptides with hydrophobic silicate nanofilms on a gold substrate. Analytical chemistry2010, 82 (22), 9211–9220. [PubMed: 20964322]
33. Xue C-H; Ma J-Z, Long-lived superhydrophobic surfaces. Journal of materials chemistry A2013, 1 (13), 4146–4161.
34. Srinivasan U; Houston MR; Howe RT; Maboudian R, Alkyltrichlorosilane-based self-assembled monolayer films for stiction reduction in silicon micromachines. Journal of Microelectromechanical Systems1998, 7 (2), 252–260.
35. Abbas A; Linman MJ; Cheng Q, Sensitivity comparison of surface plasmon resonance and plasmon-waveguide resonance biosensors. Sensors and Actuators B: Chemical2011, 156 (1), 169–175.
36. Damodaran VB; Murthy NS, Bio-inspired strategies for designing antifouling biomaterials. Biomaterials research2016, 20 (1), 18. [PubMed: 27326371]
37. Zarei M; Bindila L; Souady J; Dreisewerd K; Berkenkamp S; Müthing J; Peter-Katalinić J, A sialylation study of mouse brain gangliosides by MALDI a-TOF and o-TOF mass spectrometry. Journal of mass spectrometry2008, 43 (6), 716–725. [PubMed: 18200606]
38. Ivleva VB; Sapp LM; O'Connor PB; Costello CEGanglioside analysis by thin-layer chromatography matrix-assisted laser desorption/ionization orthogonal time-of-flight mass spectrometry. Journal of the American Society for Mass Spectrometry, 2005, 16 (9), 1552–1560. [PubMed: 16054389]
39. Chan K; Lanthier P; Liu X; Sandhu JK; Stanimirovic D; Li J, MALDI mass spectrometry imaging of gangliosides in mouse brain using ionic liquid matrix. Analytica chimica acta2009, 639 (1–2), 57–61. [PubMed: 19345758]
40. Weishaupt N; Caughlin S; Yeung KK-C; Whitehead SN, Differential anatomical expression of ganglioside GM1 species containing d18: 1 or d20: 1 sphingosine detected by MALDI imaging mass spectrometry in mature rat brain. Frontiers in neuroanatomy2015, 9, 155. [PubMed: 26648849]
41. Valdes-Gonzalez T; Goto-Inoue N; Hirano W; Ishiyama H; Hayasaka T; Setou M; Taki T, New approach for glyco-and lipidomics–Molecular scanning of human brain gangliosides by TLC-Blot and MALDI-QIT-TOF MS. Journal of neurochemistry2011, 116 (5), 678–683. [PubMed: 21244424]
42. Wood A; Chen B; Pathan S; Bok S; Mathai C; Gangopadhyay K; Grant S; Gangopadhyay S, Influence of silver grain size, roughness, and profile on the extraordinary fluorescence enhancement capabilities of grating coupled surface plasmon resonance. RSC Adv. 2015, 5 (96), 78534–78544.
43. Imberty A; Varrot A, Microbial recognition of human cell surface glycoconjugates. Current opinion in structural biology2008, 18 (5), 567–576. [PubMed: 18809496]
44. Wilkop T; Wang Z; Cheng Q, Analysis of μ-contact printed protein patterns by SPR imaging with a LED light source. Langmuir2004, 20 (25), 11141–11148. [PubMed: 15568869]

45. Phillips KS; Han J-H; Martinez M; Wang Z; Carter D; Cheng Q, Nanoscale glassification of gold substrates for surface plasmon resonance analysis of protein toxins with supported lipid membranes. Analytical chemistry2006, 78 (2), 596–603. [PubMed: 16408945]

46. Shanta PV; Li B; Stuart DD; Cheng QJAC, Plasmonic Gold Templates Enhancing Single Cell Lipidomic Analysis of Microorganisms. Analytical chemistry2020, 92 (9), 6213–6217. [PubMed: 32124608]

47. Phillips KS; Wilkop T; Wu J-J; Al-Kaysi RO; Cheng Q, Surface plasmon resonance imaging analysis of protein-receptor binding in supported membrane arrays on gold substrates with calcinated silicate films. Journal of the American Chemical Society2006, 128 (30), 9590–9591. [PubMed: 16866487]

48. Hu W; He G; Zhang H; Wu X; Li J; Zhao Z; Qiao Y; Lu Z; Liu Y; Li CMJ, Polydopamine-functionalization of graphene oxide to enable dual signal amplification for sensitive surface plasmon resonance imaging detection of biomarker. Analytical chemistry2014, 86 (9), 4488–4493. [PubMed: 24712824]

49. Koga M; Tatsumoto M; Yuki N; Hirata KJ, Range of cross reactivity of anti-GM1 IgG antibody in Guillain-Barré syndrome. J Neurol Neurosurg Psychiatry2001, 71 (1), 123–124. [PubMed: 11413278]

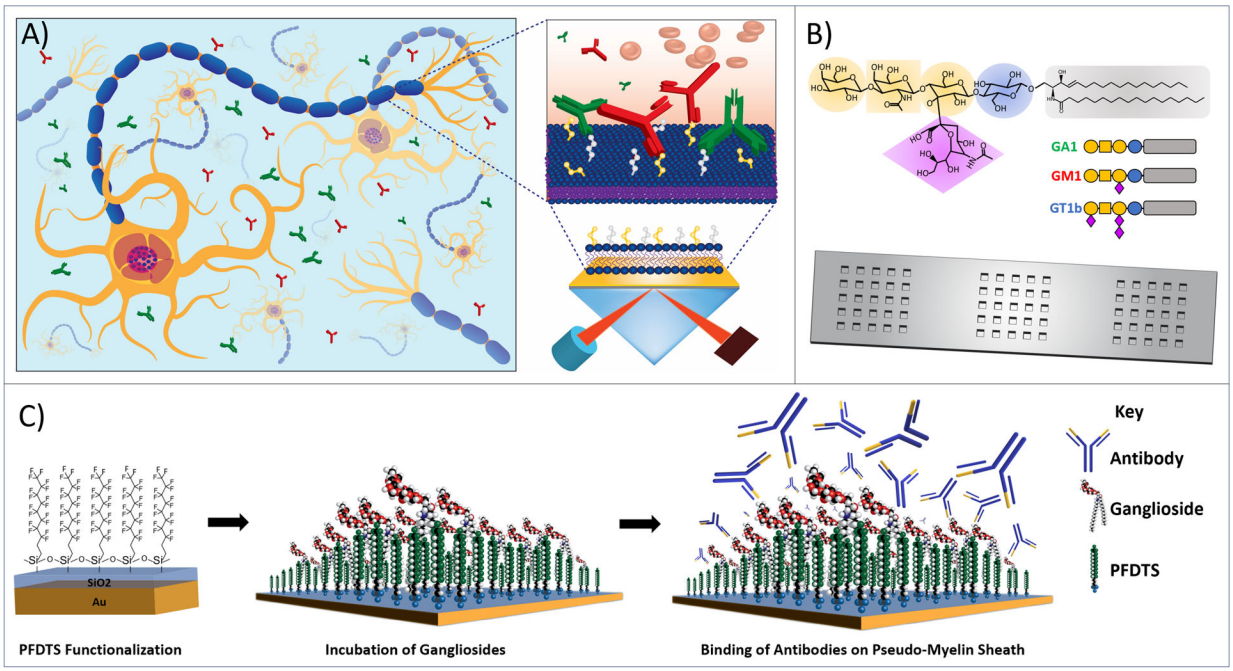

Figure 1.

(A) Cartoon illustration of MS antibody attack on the myelin sheath of nerve cells, their circulation in the blood stream and detection by an SPR sensor with a membrane-mimicking interface. (B) Structure of GM_1 ganglioside and its headgroup carbohydrates: blue circle for glucose (Glc), orange circle for galactose (Gal), orange box for N-acetylgalactosamine (GalNAC), purple diamond for N-acteylneuraminic (NeuAc); along with structures for GA_1 (green) and GT_{1b} (blue). (C) Surface functionalization steps and the detection scheme for MS specific antibodies in serum.

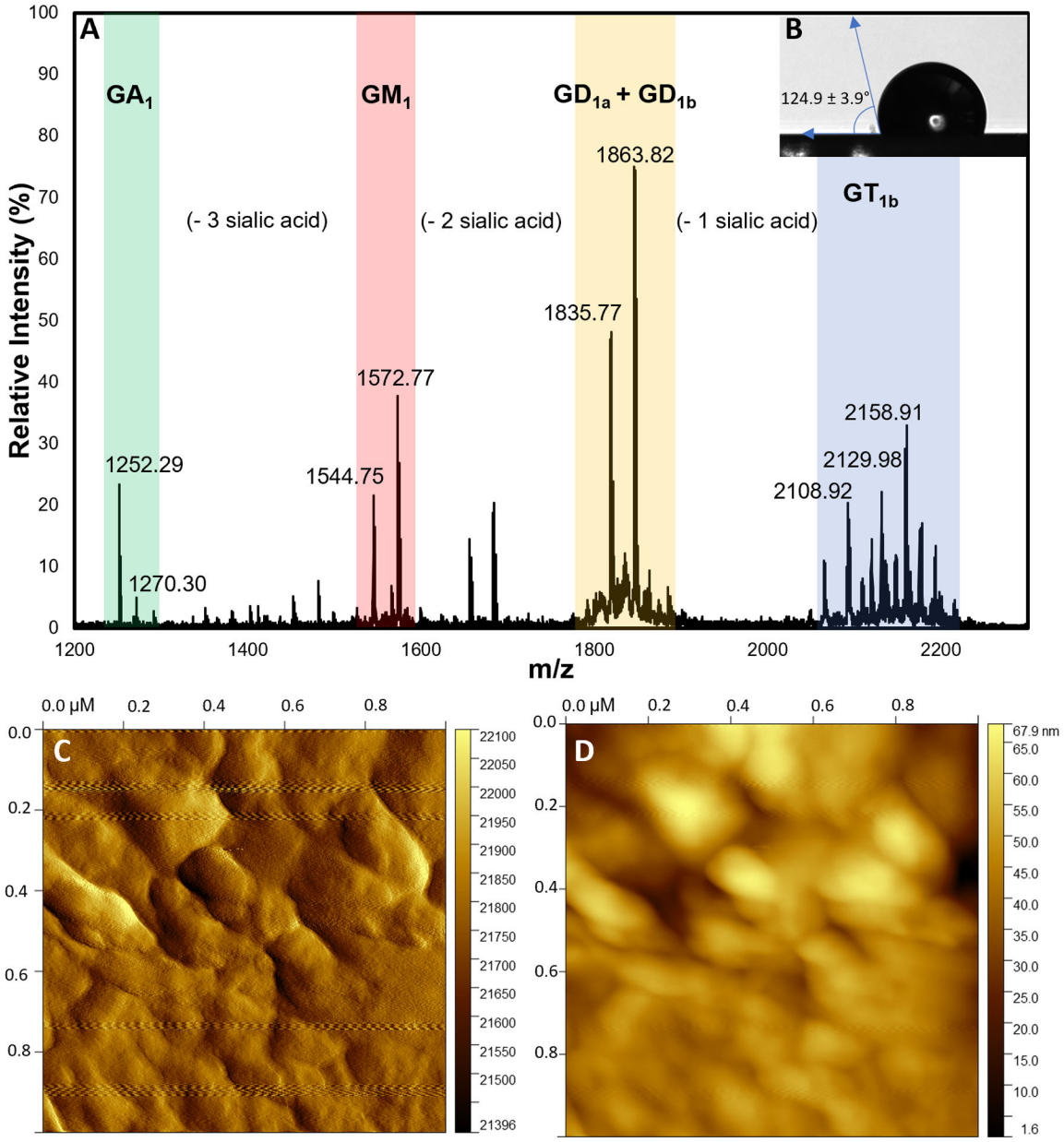

Figure 2.

(A) MALDI MS spectra for GT_{1b} ganglioside. (B) Contact angle of 0.1 mg/mL GT_{1b} ganglioside functionalized onto the PFDTS silica Au surface. (C) AFM image for 0.1 mg/mL GT_{1b} ganglioside functionalized onto the PFDTS silica Au surface and (D) a height map to show the surface roughness.

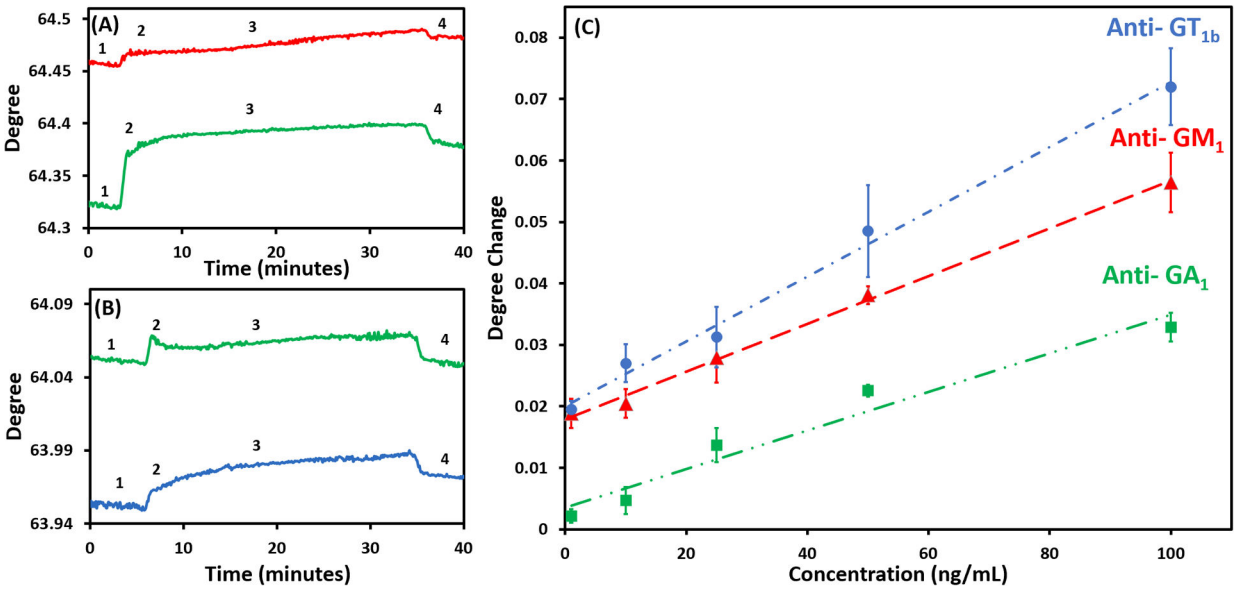

Figure 3.

Sensorgrams for (A) 50 ng/mL anti-GM_1 (Red) and 50 ng/mL anti-GA_1 (Green) in PBS on a 0.1 mg/mL GA_1 ganglioside PFDTS functionalized surface, and (B) 10 ng/mL anti-GT_{1b} (Blue) and 10 ng/mL anti-GA_1 (Green) in PBS on a GT_{1b} ganglioside PFDTS functionalized surface. Numbers indicate experimental conditions/actions for 1) Baseline, 2) Injection of antibody, 3) Incubation, and 4) Rinse. (C) calibration curves of anti-GT_{1b} (Blue), anti-GM_1 (Red), and anti-GA_1 (Green) in PBS.

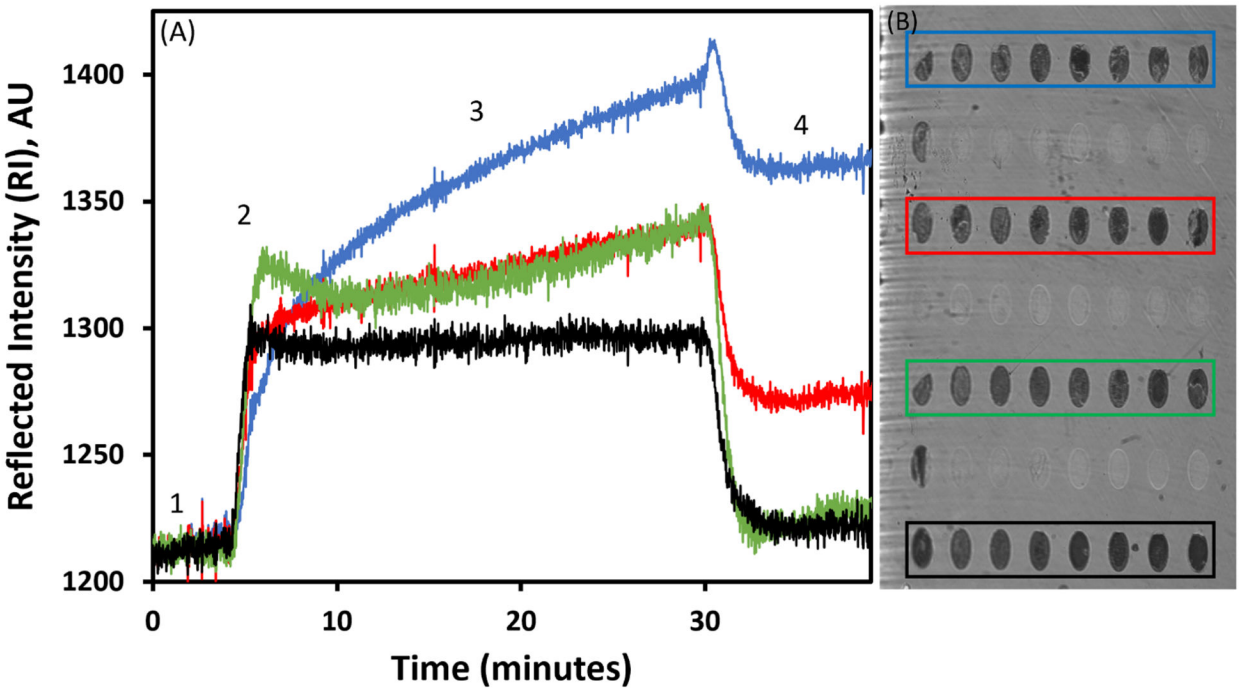

Figure 4.

(A) SPRi sensorgrams showing shifts caused by injecting 100 ng/mL anti-GT_{1b} in 10 % serum on $GT1_b$ ganglioside surface (Blue), GM_1 ganglioside surface (Red), GA_1 ganglioside surface (Green), and PFDTS surface (Black). Number indicate experimental conditions/ procedure: 1) Rinse after 10 % serum, 2) Inject 100 ng/mL anti-GT_{1b} in 10 % serum, 3) Incubation, and 4) Rinse. (B) SPR image of the ganglioside arrays. Color indicates functionalized surface in each row.

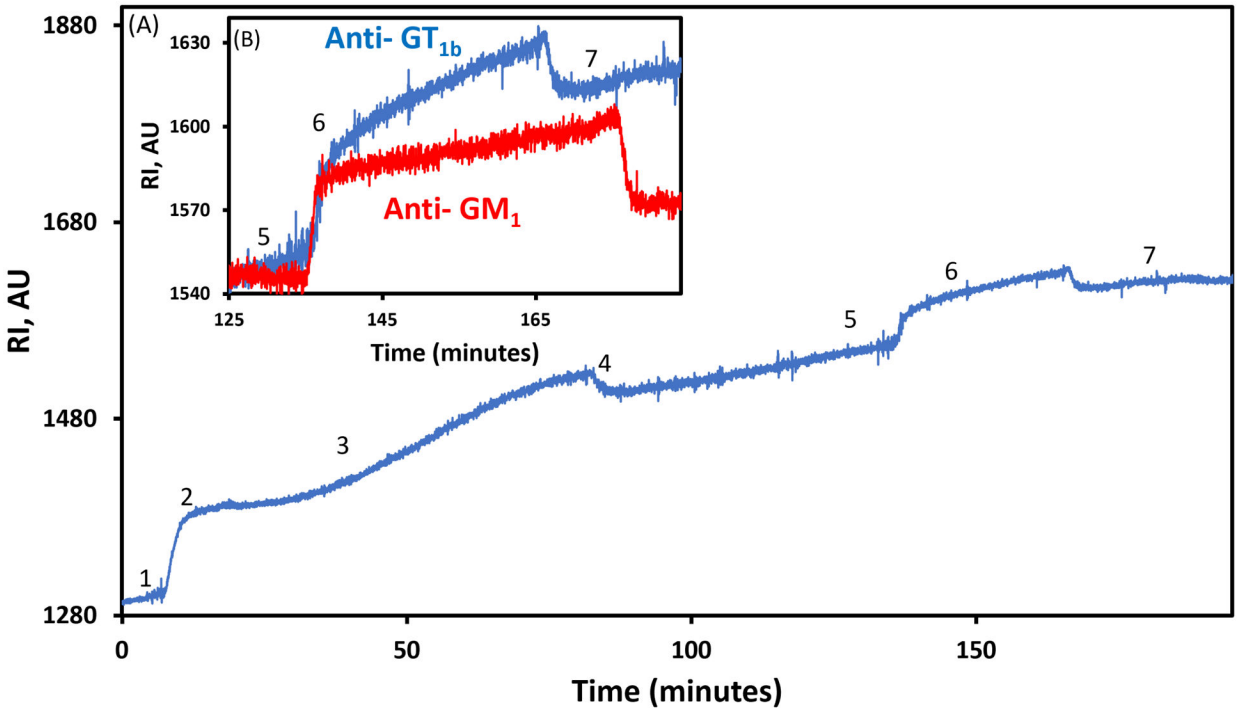

Figure 5.

(A) SPRi spectrogram of 100 ng/mL anti-GT_{1b} in 10 % serum on a PFDTS ganglioside surface (1. Baseline, 2. Injection of 10 % serum, 3. Incubation, 4. Rinse, 5. Injection of 100 ng/mL anti-GT_{1b} (Blue) and 100 ng/mL anti-GM_1 (Red) in 10 % Serum, 6. Incubation, and 7. Rinse.) (B) Cross reactivity characterized by 100 ng/mL anti-GM_1 (Red) on a GT_{1b} ganglioside functionalized surface compared to shift caused by anti-GT_{1b} (Blue).

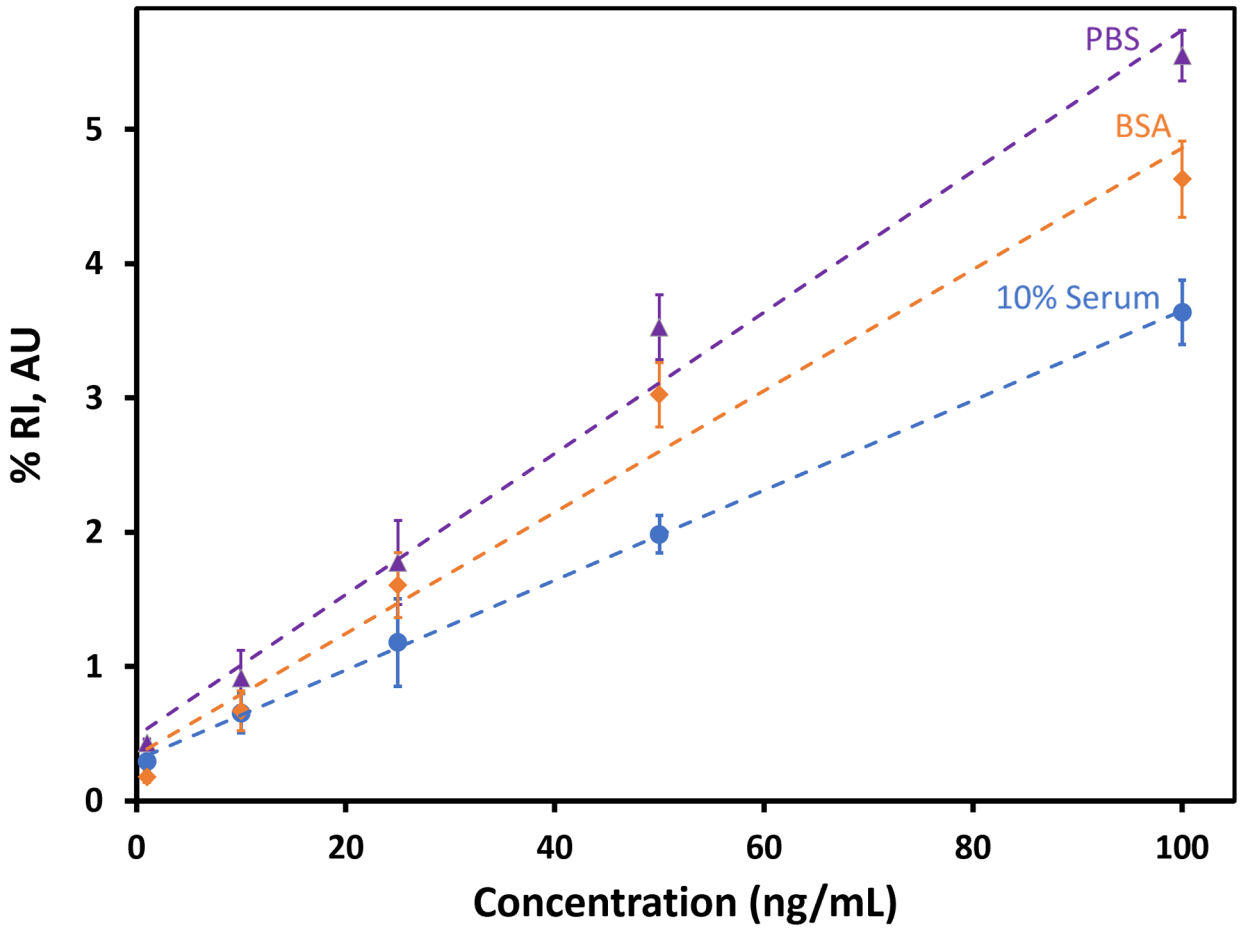

Figure 6.

Calibration curves for the specific binding between GT_{1b} ganglioside functionalized substrate and anti-GT_{1b} spiked in PBS at pH of 7.4 (purple), 2.0 mg/mL BSA (orange), and 10 % diluted serum (blue) at below (1 ng/mL) and above (20 ng/mL) MS related antibodies concentrations.

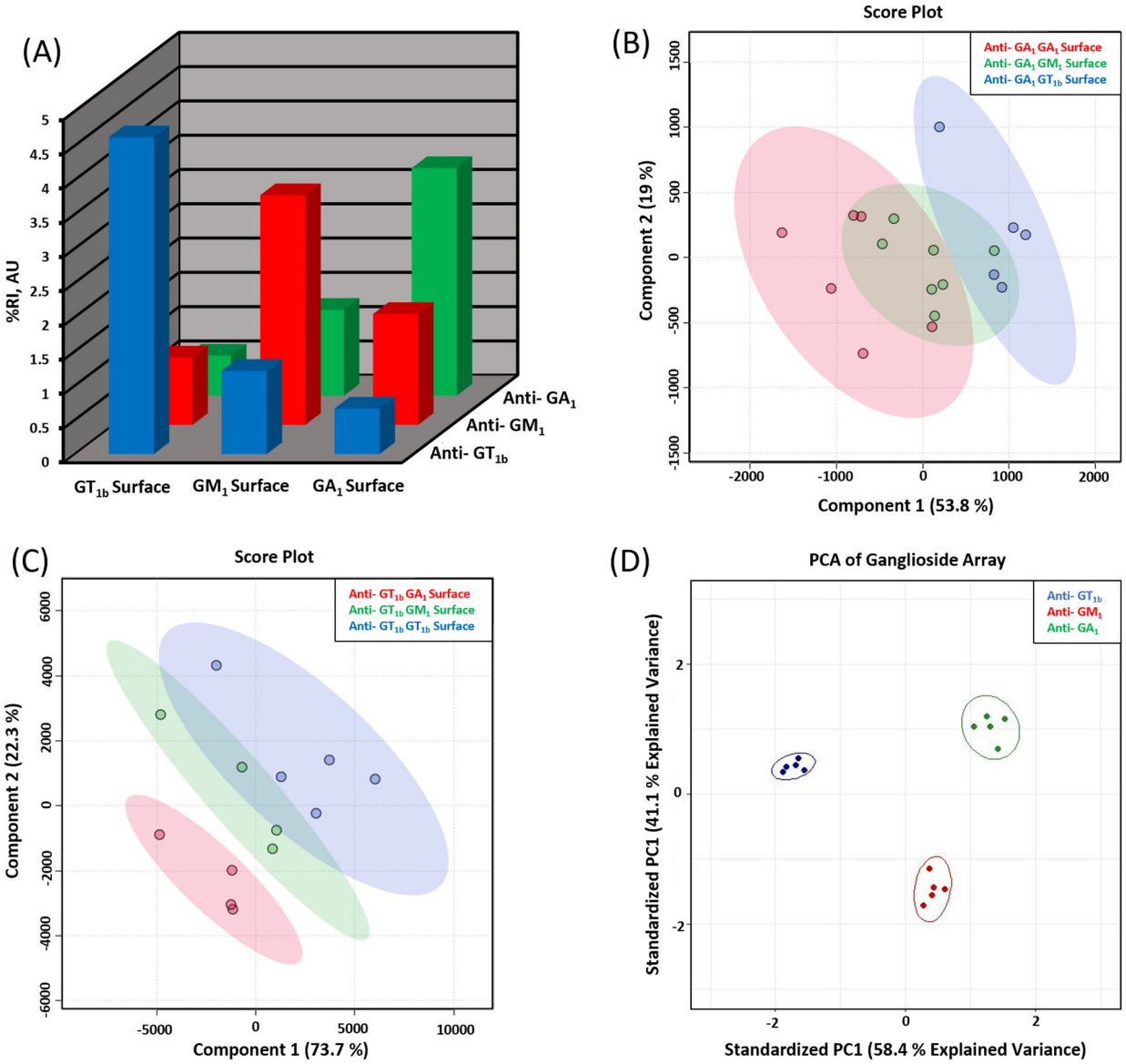

Figure 7.

(A) Bulk changes caused by MS specific antibodies at 100 ng/mL spiked in 10 % serum on a high throughput multiplexed SPRi microarray. (Blue) % RI, AU caused by 100 ng/mL anti-GT_{1b} on 0.1 mg/mL GT_{1b}, GM_1, and GA_1 ganglioside surfaces, (Red) binding between 100 ng/mL anti-GM_1 and 0.1 mg/mL on a GT_{1b}, GM_1, and GA_1 ganglioside surfaces, and (Green) binding between 100 ng/mL anti-GA_1 and 0.1 mg/mL GT_{1b}, GM_1, and GA_1 ganglioside surfaces. (B) Partial Least Squares Discriminant Analysis (PLS- DA) for 100 ng/mL anti-GA_1 on the three PFDTS ganglioside functionalized surfaces. (Red) anti-GA_1 on GA_1 ganglioside surface, (Green) anti-GA_1 on GM_1 ganglioside surface, and (Blue) anti-GA_1 on GT_{1b} ganglioside surface. (C) PLS- DA for anti-GT_{1b} on (Red) GA_1 ganglioside surface, (Green) GM_1 ganglioside surface, and (Blue) GT_{1b} ganglioside surface. (D) Principal components analysis (PCA) showing the ability to separate the three anti- ganglioside antibodies based on their induced response across the whole ganglioside

microarray. (Blue) 100 ng/mL anti-GT_{1b}, (Red) 100 ng/mL anti-GM_1, and (Green) 100 ng/mL anti-GA_1.